

Superconductivity of Incoherent Electrons near the Relativistic Mott Transition in Twisted Dirac Materials

Veronika C. Stangier,¹ Mathias S. Scheurer,² Daniel E. Sheehy,³ and Jörg Schmalian^{1,4}

¹*Institute for Theory of Condensed Matter, Karlsruhe Institute of Technology, Karlsruhe 76131, Germany*

²*Institute for Theoretical Physics III, University of Stuttgart, Stuttgart 70550, Germany*

³*Department of Physics and Astronomy, Louisiana State University, the Baton Rouge, LA 70803 USA*

⁴*Institute for Quantum Materials and Technologies, Karlsruhe Institute of Technology, Karlsruhe 76131, Germany*

(Dated: October 9, 2025)

We demonstrate that superconductivity driven by strong quantum-critical fluctuations can emerge near relativistic Mott transitions in twisted two-dimensional materials, taking on a remarkably rich character. In twisted double-bilayer WSe₂, all time-reversal-even, gap-opening collective modes promote pairing, whereas time-reversal-odd modes do not. In a Dirac model of twisted bilayer graphene, the Gross-Neveu transition into inter-valley-coherent insulators gives rise to a spectrum of degenerate and nearly degenerate superconducting states. More generally, we show that the richer the Dirac structure, the more readily pairs can form. A crucial ingredient of the theory is that critical fluctuations render the electronic states strongly incoherent, allowing attractive pairing channels to overcome the bare Dirac semi-metal behavior. Finally, we demonstrate a direct relation between boson-mediated pairing and the formation of charge-carrying skyrmionic excitations in the proximate insulating state.

Twisted two-dimensional materials have emerged as a versatile setting to study the tunable interplay of electron correlations, unconventional order and topology [1–13]. Through the control of twist angle, carrier density, and displacement fields, these systems can be driven into a remarkable variety of ordered and topological states, ranging from correlated insulators to superconductors. At the single-particle level many twisted materials possess symmetry-protected massless Dirac points. Prominent examples, where the Dirac point is right at the Fermi level, include twisted bilayer graphene (TBG) at charge neutrality [8, 10] or stacked twisted double-bilayer WSe₂ at filling $\nu = 2$ [13–17]. Increasing correlations, e.g. by changing the twist angle, tends to increase correlation effects and even open a gap at the Dirac points [6, 7, 13, 18–20]. The description of this semimetal-insulator transition in terms of the Gross-Neveu (GN) mechanism [21, 22] was shown to yield quantitative agreement for e.g. the value of the twist angle of the transition [23–26]. For such a relativistic Mott transition, the critical point represents the onset of spontaneous symmetry breaking that gaps the Dirac spectrum and is governed by strong, quantum-critical fluctuations.

In a parallel manuscript [27], we analyzed the conditions under which quantum-critical fluctuations near GN criticality can induce superconductivity at the neutrality point of a generic two-dimensional Dirac system. As illustrated in Fig. 1, strong-coupling superconductivity can emerge even though only a small number of carriers are thermally or quantum-mechanically excited. The nature of the pairing state is highly sensitive to the underlying critical bosonic mode. Remarkably, superconductivity occurs only when the fermions are sufficiently incoherent: well-defined quasi-particles remain non-superconducting, whereas strongly renormalized, ill-defined fermions are able to condense. An important open question is how the relativistic Mott transition in concrete twisted systems intertwines with this mechanism of superconductivity.

In this work, we investigate superconductivity in the vicinity of relativistic Mott transitions in twisted two-dimensional materials. To this end, we generalize and apply the theoretical

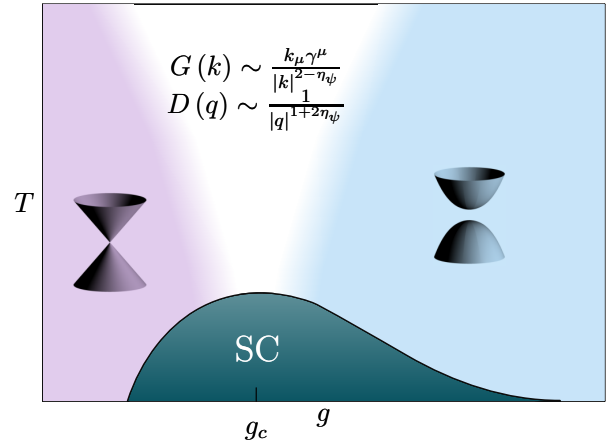


Figure 1. Schematic phase diagram for the behavior near the Gross-Neveu mass-generating transition (at g_c) of two-dimensional Dirac systems within the approach of Ref. [27]. For systems with a sufficiently large anomalous fermion dimension, η_ψ , in the electron Green's function $G(k)$, critical boson fluctuations (with propagator $D(q)$) give rise to superconductivity (SC) even in the absence of a sharp Fermi surface or any well-defined charge carriers.

framework of Ref. [27] to the concrete cases of twisted double-bilayer WSe₂ and twisted bilayer graphene (TBG). For twisted WSe₂, we demonstrate that all time-reversal-even fluctuations promote pairing, whereas time-reversal-odd fluctuations do not induce superconductivity. In TBG, focusing on inter-valley coherent insulators [28–30], we uncover a rich spectrum of degenerate and nearly degenerate superconducting states. Thus, precisely at the twist angle where the fermions become gapped, one should expect either superconductivity or, at the very least, strong pairing fluctuations. Furthermore, we establish a direct connection between our framework and the intriguing possibility of charged skyrmions as a topological mechanism for pairing [31–33], as has been intensely discussed in the context

of TBG [34–36].

We are interested in the solution of the two-dimensional coupled Dirac-fermion boson problem with Hamiltonian

$$\begin{aligned}
H = & v_F \int d^2x \psi^\dagger(\mathbf{x}) (-i\nabla) \cdot \boldsymbol{\alpha} \psi(\mathbf{x}) \\
& + \frac{1}{2} \int d^2x \sum_a \left(\pi_a^2(\mathbf{x}) + \omega_0^2 \phi_a^2(\mathbf{x}) + v_B^2 (\nabla \phi_a(\mathbf{x}))^2 \right) \\
& + g \sum_a \int d^2x \left(\psi^\dagger(\mathbf{x}) \Upsilon_a \psi(\mathbf{x}) \phi_a(\mathbf{x}) + h.c. \right). \quad (1)
\end{aligned}$$

Here ψ is an n_γ -component Dirac spinor with $\{\alpha_i, \alpha_j\} = 2\delta_{ij}$ and ϕ_a is an m_ϕ -component critical bosonic field ($a = 1 \cdots m_\phi$). π_a is its conjugate momentum. ω_0 is the bare mass of the boson, $v_{F,B}$ are the fermion and boson velocities, respectively, and g is the coupling constant, where the symmetry of the boson determines the $n_\gamma \times n_\gamma$ matrices Υ_a that act in spinor space and that have a common parity $\tau_\phi = \pm$ under time reversal.

To address the strong coupling behavior of this model at the GN critical point, we utilize a generalized Sachdev-Ye-Kitaev approach [37–40]. Following Refs. [27, 41–43] we introduce additional N fermion and M boson flavors, randomize the coupling constant g between these additional flavors, and perform a controlled large N and M expansion at fixed M/N . This theory was formulated for the normal state in Ref. [43]. The crucial aspect of the approach is that so-called melonic diagrams dominate the physical behavior. In the normal state and at the GN-critical point one obtains universal power-law behavior for the critical fermions and bosons (see Fig. 1), with a comparatively large anomalous fermion dimension $0 < \eta_\psi < \frac{1}{2}$ within a controlled theory.

To determine possible superconducting states we analyze the anomalous self energy $\Phi(k)$ in the Nambu-Gor'kov description of superconductors, which is also an $n_\gamma \times n_\gamma$ matrix in spinor space [27]. The linearized equation for $\Phi(k)$ is:

$$\Phi(k) = \frac{\lambda_p \tau_\phi}{m_\phi} \sum_{a=1}^{m_\phi} \int \frac{d^3p}{4\pi} \frac{p_\mu p_\nu \Upsilon_a \gamma^0 \gamma^\mu \Phi(p) \gamma^\nu \gamma^0 \Upsilon_a}{|p|^{4-2\eta_\psi} |k-p|^{1+2\eta_\psi}}. \quad (2)$$

At the GN-critical point, the power-law structure of the kernel and the dimensionless pairing strength

$$\lambda_p = \frac{2^{1+2\eta_\psi} (3 - \eta_\psi) \Gamma(2 - \eta_\psi) \Gamma\left(\frac{1}{2} + \eta_\psi\right) \sin(\pi\eta_\psi)}{2\pi^{3/2} (1 + \eta_\psi)} \quad (3)$$

are universally determined by the anomalous exponent η_ψ . The power laws are due to the critical behavior of the fermions and bosons while λ_p determines the degree to which the theory is strongly coupled. It vanishes if $\eta_\psi \rightarrow 0$ and is of order unity if η_ψ is no-longer small (it reaches $\frac{5}{3\pi}$ for $\eta_\psi \rightarrow \frac{1}{2}$). λ_p plays a role similar to the 't Hooft coupling [44] in the study of strongly coupled gauge theories, especially in the large- N limit.

The anomalous self energy determines the usual pairing function $\Delta(k)_{ab} \sim \langle \psi_a \psi_b \rangle$ via $\Delta(k) = \Phi(k) u_T$, where u_T is the unitary component of the time-reversal operator $\mathcal{T} = \mathcal{K} u_T^\dagger$

with complex conjugation \mathcal{K} . Fermi statistics further implies $\Delta(k) = -\Delta(-k)^T$. To determine the pairing state we expand

$$\Phi(k) = \sum_{J=1}^{n_\gamma^2} \chi_J(k) \Gamma_J, \quad (4)$$

in a complete set of Hermitian $n_\gamma \times n_\gamma$ matrices Γ_J . Only solutions that are isotropic in momentum-frequency space and hence only a function of $|k| = \sqrt{\omega^2 + \mathbf{k}^2}$ occur, where we set $v_F = 1$. The detailed $|k|$ -dependence of $\chi_J(k)$ was analyzed in Ref. [27], but will not be important for our considerations, except that $\Phi(k \rightarrow 0) \neq 0$ without fine tuning. We focus on the structure of superconductivity in spinor space. The superconducting instability only occurs for sufficiently large dimensionless pairing strength λ_p such that the normal-state anomalous dimension exceeds a critical value, i.e., $\eta_\psi \geq \eta_\psi^c$ [45]. Thus, within our theory the *incoherent* nature of electrons at criticality is essential for, and drives, superconductivity.

We now turn to the question of the Γ_J that contribute to Φ , which establish the types of pairing order that can occur. Indeed, for the dominant pairing instability of Eq. (2) this is fully determined by rather easy-to-analyze algebraic conditions [27]: It must hold that

$$\begin{aligned}
[\Gamma_J, \alpha_i] &= 0, \\
\Gamma_J \Upsilon_a &= \tau_\phi \Upsilon_a \Gamma_J, \quad (5)
\end{aligned}$$

for $i = 1, 2$ and $a = 1 \cdots m_\phi$. In addition, the pairing state must obey Fermi statistics, i.e. $(\Gamma_J u_T)^T = -\Gamma_J u_T$. If these conditions are fulfilled, superconductivity at the GN critical point will be possible. One way to interpret these conditions is that possible pairings only come from the first condition along with the Pauli condition, i.e. the possible pairings are independent of the interactions. We then use the second condition to see what couplings can create them. Assuming, for the moment, constant-in- k mean-field order parameters for superconductivity and the critical boson, the conditions of Eq. (5) imply that isotropic gaps form in the spectrum of the corresponding Bogoliubov-de Gennes Hamiltonian, where all gaps add up in squares; see appendix A. We will next scrutinize the possible pairing states and couplings compatible with Eq. (5) for twisted double-bilayer WSe_2 and TBG within their respective Dirac theories.

Twisted double-bilayer WSe_2 : Recent experiments [13] identified a semi-metal insulator transition as a function of the twist angle in AB-BA stacked twisted double-bilayer WSe_2 which is considered a strongly-correlated version of single-layer graphene [13–17] (and therefore a likely candidate for the present scenario). To apply Eq. (5) we need to identify the Dirac matrices α_i and the coupling matrices Υ_a . The relevant quantum numbers are spin, valley, and sub-lattice which we denote by the Pauli matrices σ_{j_1} , τ_{j_2} , and ρ_{j_3} , respectively. The 8×8 matrices α_i are then given by:

$$(\alpha_1, \alpha_2) = \sigma_0 (\tau_3 \rho_1, \tau_0 \rho_2). \quad (6)$$

Time-reversal is determined by $u_T = i\sigma_2 \tau_1 \rho_0$. The complete set of matrices needed for the determination of the pairing

state is most conveniently written as $\Gamma_J = \sigma_{j_1} \tau_{j_2} \rho_{j_3}$, labeled by $J = (j_1, j_2, j_3) = 1 \cdots 64$.

Let us first discuss the possible collective bosons that induce upon condensation a gap in the Dirac spectrum and whose fluctuations may serve as pairing glue. The corresponding ordered states have all been discussed in great detail, see e.g. Refs. [46–52]. Spin-orbit interaction in this system is believed to be very small [14, 15], so it is natural to consider Heisenberg couplings of the type

$$\vec{Y}_{j_2, j_3} = (Y_{1, j_2, j_3}, Y_{2, j_2, j_3}, Y_{3, j_2, j_3}) = \vec{\sigma} \tau_{j_2} \rho_{j_3}, \quad (7)$$

or coupling in the charge sector

$$Y_{0, j_2, j_3} = \sigma_0 \tau_{j_2} \rho_{j_3}. \quad (8)$$

For the combined valley and sub-lattice index (j_2, j_3) there are then in total four options that open an isotropic gap, i.e. where the coupling matrices anti-commute with α_1 and α_2 simultaneously. This is the case for $(j_2, j_3) = (0, 3), (1, 1), (2, 1),$ and $(3, 3)$. For the point group D_6 the spatial parts of these interactions transform as $B_2, A_1, B_1,$ and A_2 , respectively. The first option $Y_{\mu, 03} = \sigma_\mu \tau_0 \rho_3$ breaks the sub-lattice symmetry (either in the spin or in the charge sector). $(Y_{\mu, 11}, Y_{\mu, 21}) = \sigma_\mu (\tau_1, \tau_2) \rho_1$ are valley-mixing bond-order states akin to Kekulé order. They are closely related to the inter-valley coherent (IVC) insulators that will be discussed in the context of TBG below. Finally, $Y_{\mu, 33} = \sigma_\mu \tau_3 \rho_3$ corresponds for $\mu = 0$ to the Haldane state [53], a loop-current ordered state that breaks time-reversal symmetry, while $\vec{Y}_{33} = \vec{\sigma} \tau_3 \rho_3$ is a time-reversal even ordered state with opposite currents for the two spin flavors (parallel and anti-parallel to \vec{Y}_{33}), leading to an anomalous spin-Hall effect. Notice $\sigma_3 \tau_3 \rho_3$ is the celebrated Kane-Mele spin-orbit term [54] that would be spontaneously generated in the gapped phase.

We have analyzed all possible pairing states due to fluctuations of these collective bosons by analyzing the algebraic rules of Eq. (5) and find no stable superconducting solution due to time-reversal odd fluctuations $\vec{Y}_{03}, \vec{Y}_{11},$ and \vec{Y}_{21} . Equally, no superconductivity emerges due to fluctuations of the Haldane state $Y_{0, 33}$, also time-reversal odd. All other, time-reversal even states do, however, induce pairing: Charge-sub-lattice fluctuations with $Y_{0, 03}$ induce $\vec{\Phi} = \vec{\sigma} \tau_3 \rho_0$ which yields for the superconducting order parameter

$$\vec{\Delta}_{B_1} = i \sigma_2 \vec{\sigma} \tau_2 \rho_0, \quad (9)$$

i.e. a spin triplet, valley singlet. B_1 gives the transformation of the spatial part w.r.t. D_6 . The same coupling also induces a singlet s-wave $\Phi = \sigma_0 \tau_0 \rho_0$, which becomes

$$\Delta_{A_1} = i \sigma_2 \tau_1 \rho_0. \quad (10)$$

$\vec{\Delta}_{B_1}$ and Δ_{A_1} are, at the level of the continuum theory, degenerate; a degeneracy that will be lifted by lattice corrections to the Dirac theory.

Next, we consider valley-mixing Kekulé-type bond order fluctuation $Y_{0, 11}$ and $Y_{0, 21}$. If we consider them individually,

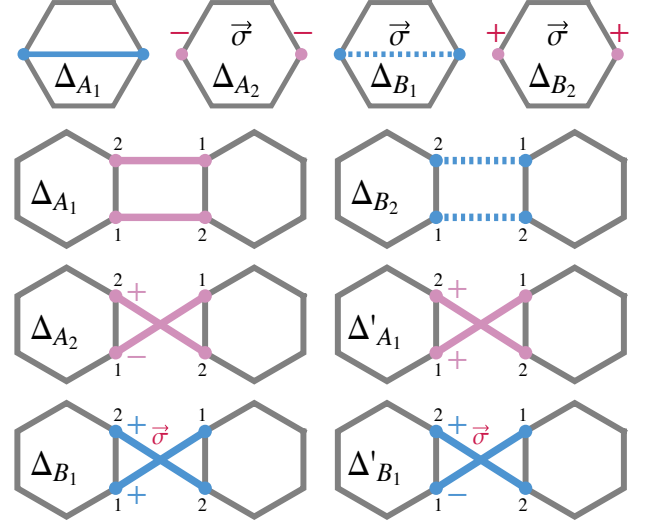


Figure 2. Top Row: The four possible SC instabilities in double-bilayer WSe₂ given in Eqs. (9), (10) and (11) labeled by the D_6 irrep. Pairing correlations that are intra-sublattice ($\propto \rho_0$) or inter-sublattice ($\propto \rho_2$) are labeled blue and pink, respectively, with solid (dashed) lines connecting inter-valley pairing of type τ_1 (τ_2). Panels with no lines indicate intravalley pairing that is either in phase ($\propto \tau_0$, indicated with +) or out of phase ($\propto \tau_3$, indicated with -). Bottom Rows: The six possible SC instabilities in TBG depending on the nature of the insulating state (KIVC or TIVC), as listed in Eqs. (15) and (16) and labeled by the D_6 irrep. In each panel the left and right hexagons are the mini-BZ's associated with opposite valleys, with numbers 1, 2 labeling mini-valleys. The valley pairing is labeled by color (pink for τ_1 and blue for τ_2). The pairing can also mix mini-valleys, with μ_1 (or μ_2) pairing given by solid (or dashed) lines, or be in the same mini-valley, with +- (or ++) labeling μ_z (or μ_0) giving the phase. In each case, $\vec{\sigma}$ indicates triplet pairing, with the other cases singlet.

as single-component order parameters, they induce either $\vec{\Phi} = \vec{\sigma} \tau_2 \rho_2$ or $\vec{\Phi} = \vec{\sigma} \tau_1 \rho_2$, which correspond to

$$\vec{\Delta}_{A_2} = i \sigma_2 \vec{\sigma} \tau_3 \rho_2 \text{ and } \vec{\Delta}_{B_2} = i \sigma_2 \vec{\sigma} \tau_0 \rho_2. \quad (11)$$

These are spin triplets and sub-lattice singlets with out-of-phase or in-phase order parameter in the valleys. They are again degenerate with the s-wave of Eq. (10). Alternatively, we can consider $(Y_{0, 11}, Y_{0, 21})$ as a degenerate two-component order parameter, a degeneracy caused by the $U_{\text{valley}}(1)$ symmetry that, within the Dirac theory, conserves charge in each valley separately. Then both spin triplets are frustrated by the other boson component, that acts pair-breaking. As a consequence, only Δ_{A_1} survives. Finally, the anomalous spin-Hall state $\vec{Y}_{33} = \vec{\sigma} \tau_3 \rho_3$ gives rise to the s-wave state Δ_{A_1} of Eq. (10). The four possible pairing states of WSe₂ are illustrated in Fig. 2 (top row).

To summarize, superconductivity at the critical twist angle for twisted double-bilayer WSe₂ occurs for bosons that do not break time-reversal symmetry. The most frequent pairing state is the s-wave of Eq. (10).

Twisted bilayer graphene: In this case we need to include, in addition to spin, valley and sub-lattice, the mini-valley quantum number (the two points \mathbf{K} and \mathbf{K}' of the mini

Brillouin zone) [23, 28, 29, 34, 55], which we denote by Pauli matrices μ_{j_4} . Hence, we now have $n_\gamma = 16$ -component Dirac spinors and will expand our pairing states in the 256 matrices $\Gamma_J = \sigma_{j_1} \tau_{j_2} \rho_{j_3} \mu_{j_4}$ and analyze the conditions in Eq. (5) to determine which of them is an allowed superconducting state. The Dirac dispersion is described by the two Dirac matrices

$$(\alpha_1, \alpha_2) = \sigma_0 (\tau_3 \rho_1, \tau_0 \rho_2) \mu_0. \quad (12)$$

Time reversal is determined by $u_T = i\sigma_2 \tau_1 \rho_0 \mu_0$. For simplicity we focus on bosons that yield IVC insulators, i.e. that break the translation invariance of the original graphene lattice by forming bond- or loop-current order [29, 55] and that have been observed, albeit at different fillings [56]. The effects of all other gap-inducing bosons for TBG are listed in appendix A. The coupling of Dirac fermions to an IVC state depends on whether it does or does not break time-reversal symmetry [26, 57]. In the former case we have the Kramers-IVC (KIVC) with coupling matrices

$$(\Upsilon_1, \Upsilon_2)_{\text{KIVC}} = \sigma_0 (\tau_1, \tau_2) \rho_1 \mu_2, \quad (13)$$

or, alternatively, the time-reversal symmetric IVC (TIVC) with

$$(\Upsilon_1, \Upsilon_2)_{\text{TIVC}} = \sigma_0 (\tau_1, \tau_2) \rho_1 \mu_1. \quad (14)$$

In appendix A we discuss similar results for other TIVC states. In both cases we consider a two-component or XY -order parameter.

For both interactions we find from the algebraic conditions, Eq. (5) four degenerate pairing solutions. In the case of KIVC they are

$$\begin{aligned} \Delta_{A_1} &\propto i\sigma_2 \tau_1 \rho_0 \mu_1, \\ \Delta_{A_2} &\propto i\sigma_2 \tau_1 \rho_0 \mu_3, \\ \vec{\Delta}_{B_1} &\propto i\sigma_2 \vec{\sigma} \tau_2 \rho_0 \mu_0, \\ \Delta_{B_2} &\propto i\sigma_2 \tau_2 \rho_0 \mu_2. \end{aligned} \quad (15)$$

Except for the spin triplet B_1 state, all of these superconductors are spin singlets. While the A_1 order parameter transforms trivially under all point group symmetries, it corresponds to a finite-momentum superconductor with non-trivial phase shift under moiré translation; this is also true for B_2 in Eq. (15) while the remaining two states have Cooper pairs with zero center-of-mass momentum.

Considering TIVC fluctuations, Δ_{A_1} and Δ_{B_2} are unchanged while instead of the other two, we now find

$$\begin{aligned} \Delta'_{A_1} &\propto i\sigma_2 \tau_1 \rho_0 \mu_0, \\ \vec{\Delta}'_{B_1} &\propto i\sigma_2 \vec{\sigma} \tau_2 \rho_0 \mu_3. \end{aligned} \quad (16)$$

These four states are again degenerate at the level of the Dirac theory. The six distinct pairing states of TBG, discussed above, are illustrated in Fig. 2 (bottom three rows). Most importantly, in TBG we find superconductivity emerging at the onset of inter-valley coherent insulators, irrespective of whether time-reversal symmetry is broken or preserved. The additional mini-valley flavor structure substantially enhances the range of possible pairing states, in comparison to WSe₂.

To estimate the superconducting transition temperature T_c in these twisted Dirac materials, we note that the maximal T_c obtained in Ref. [27] is approximately $2 \times 10^{-3} \Lambda$, where Λ denotes the cutoff energy of the Dirac model. For both WSe₂ at a twist angle of $\theta \approx 2.7^\circ$ and for TBG at $\theta \approx 1.2^\circ$ one finds $\Lambda \sim 20 \text{ meV}$ [13, 20], which yields an optimal transition temperature of $T_c \approx 0.4 \text{ K}$.

For both systems, our results for pairing at the semi-metal to insulator transition were obtained in the limit where we only consider the Dirac point and ignore the behavior in the rest of the mini-Brillouin zone or due to higher bands. Hence, we should ask: Are there implications beyond the Dirac physics near the Gross-Neveu critical point? In this context, it is interesting that the second condition in Eq. (5) was recently obtained in the study of pairing instabilities of TBG in the extreme flat-band limit [58], i.e. not in the Dirac regime. This strongly suggests that it may in fact be of more general relevance than either limit. Of course, the first condition in Eq. (5) is specific to the Dirac theory.

Of the many approaches to link superconductivity to nearby ordered states, a particularly beautiful and powerful one is the observation that the seeds of pairing are planted in the topological excitations of the insulator and vice versa [31–36]. This is the result of a Wess-Zumino-Witten term

$$S_{\text{WZW}} = i \frac{3\mathcal{N}}{4\pi} \int \epsilon_{\alpha\beta\gamma\delta\nu} n_\alpha \partial_u n_\beta \partial_\tau n_\gamma \partial_x n_\delta \partial_y n_\nu, \quad (17)$$

of the coupled superconducting and mass-generating boson problem. The five-component order parameter n_α comprises the two components of the complex superconducting order parameter together with three suitably chosen collective bosonic modes, denoted by \vec{Y} . The integration $\int \dots = \int d^3x \int_0^1 du$ extends over space-time and the auxiliary variable u [31–36]. Ref. [34] formulated three conditions for $\mathcal{N} \neq 0$ in a particularly convenient way for our purposes. Remarkably, the pairing conditions of Eq. (5), derived from the analysis of the critical pairing problem, coincide with two of these three criteria. The remaining condition imposes an additional constraint on the three components of \vec{Y} , namely

$$\text{tr}(\alpha_{i_1} \alpha_{i_2} \Upsilon_{a_1} \Upsilon_{a_2} \Upsilon_{a_3}) = -8\mathcal{N} \epsilon_{i_1 i_2 a_1 a_2 a_3} \neq 0, \quad (18)$$

which also determines the coefficient \mathcal{N} in Eq. (17).

Analyzing options for such topologically enabled pairing for WSe₂, we find the partner states $\vec{Y} = (\Upsilon_{011}, \Upsilon_{021}, \Upsilon_{003})$ and \vec{Y}_{33} , both with Δ_{A_1} of Eq. (10). Hence, either a combination of bond with charge order or the anomalous spin-Hall state, already discussed in Ref. [33], form natural partner orders with s -wave superconductivity to yield a topological origin of pairing. Here $\mathcal{N} = 1$ and skyrmion defects in the insulator carry charge $2e$. For the TBG problem, the behavior is again much richer and we find in total 56 such partner states, all combined with a wide array of superconducting states. They are listed in appendix B, see also Ref. [34]. Examples are the two states for WSe₂ multiplied by the unit matrix in mini-valley space: $\vec{Y}\mu_0$ and $\vec{Y}_{33}\mu_0$. As a result of the additional mini-valley quantum number, we have $\mathcal{N} = 2$ so that skyrmions carry charge $4e$. For both systems, we find the common theme

that only bosons that are even under time-reversal yield non-zero S_{WZW} .

These results are rather unexpected. *A priori*, there is no reason to expect a connection between the conditions arising from a pairing instability due to critical boson exchange and those required for a topological term in the action. Yet our analysis implies that all insulators with charged skyrmions, together with their superconducting partners, form a subset of the states we obtain from Eq. (5). Moreover, our theory shows not only that these particle-hole / particle-particle partners are natural candidates for topological pairing, but also that the superconducting partners are in fact induced by fluctuations of particle-hole modes. Consequently, the pairing states obtained here may be of significance even beyond neutrality or the specific critical point analyzed.

In summary, we investigate superconductivity emerging near relativistic Mott transitions in twisted two-dimensional Dirac materials. Using a controlled strong-coupling framework, based on a generalized Sachdev-Ye-Kitaev approach, it was shown in Ref. [27] that superconductivity may appear once the fermionic anomalous dimension induced by Gross–Neveu criticality exceeds a universal threshold, enabling attractive pairing to overcome the bare Dirac semi-metal behavior. Applying this theory to twisted double-bilayer WSe_2 , we find that all time-reversal even bosons cause superconductivity. In contrast, for TBG we find a manifold of degenerate and nearly

degenerate superconducting states that can be either time-reversal even or odd. Broadly speaking, the more intricate the Dirac structure (i.e., the larger the Dirac representation of the twisted material), the more readily pairs can form. Finally, we established a direct link between pairing due to critical bosons and the formation of charged topological solitons, i.e. skyrmions, in the associated insulator. The latter are a subset of the former. Twisted Dirac materials provide a controlled and tunable setting to probe the interplay between relativistic Mott criticality, the associated insulating states, and unconventional superconductivity.

We are grateful to Andrey V. Chubukov, Laura Classen, Elio König, and Nikolaos Parthenios for helpful discussions. This work was supported by the German Research Foundation TRR 288-422213477 ELASTO-Q-MAT, B01 (V.C.S. and J.S.) and grant SFI-MPS- NFS-00006741-05 from the Simons Foundation (J.S.). D.E.S. acknowledges support from the National Science Foundation under Grant PHY-2208036. M.S.S. acknowledges funding by the European Union (ERC-2021-STG, Project 101040651—SuperCorr). Views and opinions expressed are however those of the authors only and do not necessarily reflect those of the European Union or the European Research Council Executive Agency. Neither the European Union nor the granting authority can be held responsible for them.

-
- [1] G. Li, A. Luican, J. Lopes dos Santos, A. Castro Neto, A. Reina, J. Kong, and E. Andrei, *Nature physics* **6**, 109 (2010).
- [2] Y. Cao, V. Fatemi, A. Demir, S. Fang, S. L. Tomarken, J. Y. Luo, J. D. Sanchez-Yamagishi, K. Watanabe, T. Taniguchi, E. Kaxiras, *et al.*, *Nature* **556**, 80 (2018).
- [3] Y. Cao, V. Fatemi, S. Fang, K. Watanabe, T. Taniguchi, E. Kaxiras, and P. Jarillo-Herrero, *Nature* **556**, 43 (2018).
- [4] E. Y. Andrei and A. H. MacDonald, *Nature materials* **19**, 1265 (2020).
- [5] M. Yankowitz, S. Chen, H. Polshyn, Y. Zhang, K. Watanabe, T. Taniguchi, D. Graf, A. F. Young, and C. R. Dean, *Science* **363**, 1059 (2019).
- [6] X. Lu, P. Stepanov, W. Yang, M. Xie, M. A. Aamir, I. Das, C. Urgell, K. Watanabe, T. Taniguchi, G. Zhang, *et al.*, *Nature* **574**, 653 (2019).
- [7] Y. Xie, B. Lian, B. Jäck, X. Liu, C.-L. Chiu, K. Watanabe, T. Taniguchi, B. A. Bernevig, and A. Yazdani, *Nature* **572**, 101 (2019).
- [8] A. Kerelsky, L. J. McGilly, D. M. Kennes, L. Xian, M. Yankowitz, S. Chen, K. Watanabe, T. Taniguchi, J. Hone, C. Dean, *et al.*, *Nature* **572**, 95 (2019).
- [9] M. Serlin, C. Tschirhart, H. Polshyn, Y. Zhang, J. Zhu, K. Watanabe, T. Taniguchi, L. Balents, and A. Young, *Science* **367**, 900 (2020).
- [10] U. Zondiner, A. Rozen, D. Rodan-Legrain, Y. Cao, R. Queiroz, T. Taniguchi, K. Watanabe, Y. Oreg, F. von Oppen, A. Stern, *et al.*, *Nature* **582**, 203 (2020).
- [11] L. Balents, C. R. Dean, D. K. Efetov, and A. F. Young, *Nature Physics* **16**, 725 (2020).
- [12] D. M. Kennes, M. Claassen, L. Xian, A. Georges, A. J. Millis, J. Hone, C. R. Dean, D. Basov, A. N. Pasupathy, and A. Rubio, *Nature Physics* **17**, 155 (2021).
- [13] L. Ma, R. Chaturvedi, P. X. Nguyen, K. Watanabe, T. Taniguchi, K. F. Mak, and J. Shan, *arXiv preprint arXiv:2412.07150* (2024).
- [14] M. Angeli and A. H. MacDonald, *Proceedings of the National Academy of Sciences* **118**, e2021826118 (2021).
- [15] H. Pan, E.-A. Kim, and C.-M. Jian, *Physical Review Research* **5**, 043173 (2023).
- [16] B. A. Foutty, J. Yu, T. Devakul, C. R. Kometter, Y. Zhang, K. Watanabe, T. Taniguchi, L. Fu, and B. E. Feldman, *Nature Materials* **22**, 731 (2023).
- [17] M. Tolosa-Simeón, L. Classen, and M. M. Scherer, *Physical Review B* **112**, 115133 (2025).
- [18] Y. Choi, J. Kemmer, Y. Peng, A. Thomson, H. Arora, R. Polski, Y. Zhang, H. Ren, J. Alicea, G. Refael, *et al.*, *Nature physics* **15**, 1174 (2019).
- [19] P. Stepanov, I. Das, X. Lu, A. Fahimniya, K. Watanabe, T. Taniguchi, F. H. Koppens, J. Lischner, L. Levitov, and D. K. Efetov, *Nature* **583**, 375 (2020).
- [20] J. Xiao, A. Inbar, J. Birkbeck, N. Gershon, Y. Zamir, T. Taniguchi, K. Watanabe, E. Berg, and S. Ilani, *arXiv preprint arXiv:2506.20738* (2025).
- [21] D. J. Gross and A. Neveu, *Physical Review D* **10**, 3235 (1974).
- [22] J. Zinn-Justin, *Nuclear Physics B* **367**, 105 (1991).
- [23] N. Parthenios and L. Classen, *Phys. Rev. B* **108**, 235120 (2023).
- [24] J. Biedermann and L. Janssen, *Phys. Rev. B* **112**, L041109 (2025).
- [25] B. Hawashin, M. M. Scherer, and L. Janssen, *Phys. Rev. B* **111**, 205129 (2025).
- [26] C. Huang, N. Parthenios, M. Ulybyshev, X. Zhang, F. F. Assaad, L. Classen, and Z. Y. Meng, *Nature Communications* **16**, 7176

- (2025).
- [27] V. C. Stangier, D. E. Sheehy, and J. Schmalian, (2025), [arXiv:2509.25318 \[cond-mat.str-el\]](https://arxiv.org/abs/2509.25318).
 - [28] H. C. Po, L. Zou, A. Vishwanath, and T. Senthil, *Phys. Rev. X* **8**, 031089 (2018).
 - [29] N. Bultinck, E. Khalaf, S. Liu, S. Chatterjee, A. Vishwanath, and M. P. Zaletel, *Phys. Rev. X* **10**, 031034 (2020).
 - [30] S. Liu, E. Khalaf, J. Y. Lee, and A. Vishwanath, *Phys. Rev. Res.* **3**, 013033 (2021).
 - [31] P. B. Wiegmann, *Phys. Rev. B* **59**, 15705 (1999).
 - [32] A. Abanov and P. B. Wiegmann, *Nuclear Physics B* **570**, 685 (2000).
 - [33] T. Grover and T. Senthil, *Phys. Rev. Lett.* **100**, 156804 (2008).
 - [34] M. Christos, S. Sachdev, and M. S. Scheurer, *Proceedings of the National Academy of Sciences* **117**, 29543 (2020).
 - [35] E. Khalaf, S. Chatterjee, N. Bultinck, M. P. Zaletel, and A. Vishwanath, *Science Advances* **7**, eabf5299 (2021).
 - [36] P. J. Ledwith, E. Khalaf, and A. Vishwanath, *Annals of Physics* **435**, 168646 (2021).
 - [37] S. Sachdev and J. Ye, *Phys. Rev. Lett.* **70**, 3339 (1993).
 - [38] A. Georges, O. Parcollet, and S. Sachdev, *Phys. Rev. Lett.* **85**, 840 (2000).
 - [39] S. Sachdev, *Phys. Rev. Lett.* **105**, 151602 (2010).
 - [40] A. Kitaev, *Talks at KITP, University of California, Santa Barbara, Entanglement in Strongly-Correlated Quantum Matter* (2015).
 - [41] I. Esterlis and J. Schmalian, *Phys. Rev. B* **100**, 115132 (2019).
 - [42] Y. Wang, *Phys. Rev. Lett.* **124**, 017002 (2020).
 - [43] J. Kim, E. Altman, and X. Cao, *Physical Review B* **103**, L081113 (2021).
 - [44] G. 't Hooft, *Nuclear Physics B* **73**, 461 (1974).
 - [45] While $\eta_{\psi}^c \approx 0.14628$ within our theory [27], we regard the *existence* of such a minimum anomalous fermion dimension (rather than its precise value, which will depend on details beyond the scope of our analysis) as the key prediction of our theory.
 - [46] I. F. Herbut, *Physical Review Letters* **97**, 146401 (2006).
 - [47] I. F. Herbut, V. Juričić, and B. Roy, *Phys. Rev. B* **79**, 085116 (2009).
 - [48] I. F. Herbut, V. Juričić, and O. Vafek, *Phys. Rev. B* **80**, 075432 (2009).
 - [49] V. Juričić, I. F. Herbut, and G. W. Semenoff, *Phys. Rev. B* **80**, 081405 (2009).
 - [50] C. Weeks and M. Franz, *Phys. Rev. B* **81**, 085105 (2010).
 - [51] G. W. Semenoff, *Physica Scripta* **2012**, 014016 (2012).
 - [52] F. F. Assaad and I. F. Herbut, *Physical Review X* **3**, 031010 (2013).
 - [53] F. D. M. Haldane, *Phys. Rev. Lett.* **61**, 2015 (1988).
 - [54] C. L. Kane and E. J. Mele, *Phys. Rev. Lett.* **95**, 226801 (2005).
 - [55] J. Kang and O. Vafek, *Phys. Rev. Lett.* **122**, 246401 (2019).
 - [56] K. P. Nuckolls, R. L. Lee, M. Oh, D. Wong, T. Soejima, J. P. Hong, D. Călugăru, J. Herzog-Arbeitman, B. A. Bernevig, K. Watanabe, *et al.*, *Nature* **620**, 525 (2023).
 - [57] J. Ingham, T. Li, M. S. Scheurer, and H. D. Scammell, *arXiv preprint arXiv:2308.00748* (2023).
 - [58] M. Christos, S. Sachdev, and M. S. Scheurer, *Nature Communications* **14**, 7134 (2023).

Appendix A: Interpretation of the pairing conditions and lists of pairing states

To interpret the conditions in Eq. (5) of the main paper physically, we assume for simplicity $\Phi(k) = \chi \Gamma_J$ with χ a constant function of k and consider finite expectation values $\mu_a \sim \langle \phi_a \rangle$. The normal state Hamiltonian becomes $h_{\mathbf{k}} = v_F \mathbf{k} \cdot \boldsymbol{\alpha} + \mu_a \Upsilon_a$ which yields the Bogoliubov-de Gennes Hamiltonian

$$\mathcal{H}_{\mathbf{k}}^{\text{BdG}} = \begin{pmatrix} h_{\mathbf{k}} & \Phi_{\mathbf{k}} \\ \Phi_{\mathbf{k}}^\dagger & -u_T^\dagger h_{-\mathbf{k}}^* u_T \end{pmatrix} = v_F \mathbf{k} \cdot \tilde{\boldsymbol{\alpha}} + \sum_{r=1}^{m_\phi+2} \mu_r \tilde{\beta}_r, \quad (\text{A1})$$

with $\tilde{\alpha}_i = \alpha_i \kappa_z$ and additional Pauli matrices κ_a in Nambu space. The masses $\mu_r = (\mu_1, \dots, \mu_{m_\phi}, \text{Re}\chi, -\text{Im}\chi)$ are either due to the condensation of the bosonic mode or the superconducting order parameter. For $1 \leq r \leq m_{m_\phi}$ holds $\tilde{\beta}_r = \Upsilon_r \kappa_z$ if $\tau_\phi = 1$ or $\tilde{\beta}_r = \Upsilon_r \kappa_0$ if $\tau_\phi = -1$. In addition $\tilde{\beta}_{r=m_\phi+1} = \Gamma_J \kappa_x$ and $\tilde{\beta}_{r=m_\phi+2} = \Gamma_J \kappa_y$ describe the superconducting gap. The conditions, Eq. (5) then become $\{\tilde{\beta}_r, \tilde{\beta}_{r'}\} = \delta_{r,r'}$ and $\{\tilde{\alpha}_i, \tilde{\beta}_{r'}\} = 0$. Hence all mass terms add in squares with Bogoliubov energies $E_{\mathbf{k}} = \pm \sqrt{(v_F \mathbf{k})^2 + \sum_r \mu_r^2}$.

Finally, we list all pairing states for the Dirac theories of twisted double bilayer WSe₂ and twisted bilayer graphene. The algebraic conditions for pairing are given in Eq. (5). The pairing states for AB-BA stacked twisted double-bilayer WSe₂ at filling $\nu = 2$ are listed in Table I, while the states for twisted bilayer graphene are listed in Table II.

Appendix B: List of partner states

In this section we list all bosonic parts of the partner states that give rise to a Wess-Zumino-Witten term S_{WZW} in the action. Conditions for the presence of S_{WZW} of the coupled superconducting and mass-generating boson problem were listed in Ref. [34] (see Eqs.(14a)-(14c) of Ref. [34]), which in our notation corresponds to:

$$\begin{aligned} \alpha_i \Gamma_J u_T^\dagger &= -\Gamma_J u_T^\dagger \alpha_i^T \neq 0 \text{ for } i = 1, 2 \\ \Upsilon_l \Gamma_J u_T^\dagger &= \Gamma_J u_T^\dagger \Upsilon_l^T \neq 0 \text{ for } l = 1, 2, 3 \\ \text{tr}(\alpha_{i_1} \alpha_{i_2} \Upsilon_{l_1} \Upsilon_{l_2} \Upsilon_{l_3}) &\propto \epsilon_{i_1 i_2 l_1 l_2 l_3} \neq 0. \end{aligned} \quad (\text{B1})$$

With $u_T^\dagger \alpha_i^T u_T = -\alpha_i$, we rewrite the first equation as $\alpha_i \Gamma_J = \Gamma_J \alpha_i$, which is the first condition Eq. (5) of the main text. With $u_T^\dagger \Upsilon_l^T u_T = \tau \Upsilon_l$, the second line in Eq. (B1) becomes $\Upsilon_l \Gamma_J = \tau \Gamma_J \Upsilon_l$, which is precisely the second condition in Eq. (5) of the main text. Hence, terms that give rise to a WZW term are a subset of those that make up the pairing states of our Dirac theory. To identify this subset, we need to analyze the last condition in Eq. (B1).

Performing this analysis for the Dirac theory of WSe₂ we find 20 triples that obey Eq. (B1). Each of them gives rise to a nontrivial pairing state. If we consider only those where all three components transform the same under time reversal, there are only two such options left and both are even under

time reversal. They are the anomalous spin-Hall state

$$\tilde{\Upsilon}_{33} = \sigma \tau_3 \rho_3, \quad (\text{B2})$$

and the combination

$$\tilde{\Upsilon} = \sigma_0 (\tau_1 \rho_1, \tau_2 \rho_1, \tau_0 \rho_3) \quad (\text{B3})$$

of the TIVC XY-state and charge sub-lattice order. Both were also listed in the main text. The superconducting partner state is $\Phi \sim e^{i\theta} \sigma_0 \tau_0 \rho_0$

Looking for triples of order parameters that obey Eq. (B1) for the Dirac model of twisted bilayer graphene, we find in total 336 distinct triples. If we confine ourselves again to the ones where all three components of the order parameter transform the same under time reversal we find 56 triples. They are also all even under time reversal and given by

$$\begin{aligned} \tilde{\Upsilon}_1 &= \sigma_0 (\tau_1 \rho_1, \tau_2 \rho_1, \tau_0 \rho_3) \mu_0 \\ \tilde{\Upsilon}_2 &= \sigma_0 (\tau_1 \rho_1 \mu_0, \tau_2 \rho_1 \mu_1, \tau_0 \rho_3 \mu_1) \\ \tilde{\Upsilon}_{3-5} &= (\sigma_0 \tau_1 \rho_1 \mu_0, \sigma_i \tau_2 \rho_1 \mu_2, \sigma_i \tau_0 \rho_3 \mu_2) \\ \tilde{\Upsilon}_6 &= \sigma_0 (\tau_1 \rho_1 \mu_0, \tau_2 \rho_1 \mu_3, \tau_0 \rho_3 \mu_3) \\ \tilde{\Upsilon}_7 &= \sigma_0 (\tau_2 \rho_1 \mu_0, \tau_1 \rho_1 \mu_1, \tau_0 \rho_3 \mu_1) \\ \tilde{\Upsilon}_{8-10} &= (\sigma_0 \tau_2 \rho_1 \mu_0, \sigma_i \tau_1 \rho_1 \mu_2, \sigma_i \tau_0 \rho_3 \mu_2) \\ \tilde{\Upsilon}_{11} &= \sigma_0 (\tau_2 \rho_1 \mu_0, \tau_1 \rho_1 \mu_3, \tau_0 \rho_3 \mu_3) \\ \tilde{\Upsilon}_{12} &= \sigma_0 (\tau_1 \rho_1 \mu_1, \tau_2 \rho_1 \mu_1, \tau_0 \rho_3 \mu_0) \\ \tilde{\Upsilon}_{13-15} &= (\sigma_0 \tau_0 \rho_3 \mu_0, \sigma_i \tau_1 \rho_1 \mu_2, \sigma_i \tau_2 \rho_1 \mu_2) \\ \tilde{\Upsilon}_{16} &= \sigma_0 (\tau_1 \rho_1 \mu_3, \tau_2 \rho_1 \mu_3, \tau_0 \rho_3 \mu_0) \\ \tilde{\Upsilon}_{17} &= (\sigma_1, \sigma_2, \sigma_3) \tau_3 \rho_3 \mu_0 \\ \tilde{\Upsilon}_{18} &= (\sigma_1 \tau_3 \rho_3 \mu_0, \sigma_2 \tau_3 \rho_3 \mu_1, \sigma_3 \tau_3 \rho_3 \mu_1) \\ \tilde{\Upsilon}_{19} &= (\sigma_1 \tau_3 \rho_3 \mu_0, \sigma_2 \tau_1 \rho_1 \mu_2, \sigma_3 \tau_1 \rho_1 \mu_2) \\ \tilde{\Upsilon}_{20} &= (\sigma_1 \tau_3 \rho_3 \mu_0, \sigma_2 \tau_2 \rho_1 \mu_2, \sigma_3 \tau_2 \rho_1 \mu_2) \\ \tilde{\Upsilon}_{21} &= (\sigma_1 \tau_3 \rho_3 \mu_0, \sigma_2 \tau_0 \rho_3 \mu_2, \sigma_3 \tau_0 \rho_3 \mu_2) \\ \tilde{\Upsilon}_{22} &= (\sigma_1 \tau_3 \rho_3 \mu_0, \sigma_2 \tau_3 \rho_3 \mu_3, \sigma_3 \tau_3 \rho_3 \mu_3) \\ \tilde{\Upsilon}_{23} &= (\sigma_1 \tau_3 \rho_3 \mu_1, \sigma_2 \tau_3 \rho_3 \mu_0, \sigma_3 \tau_3 \rho_3 \mu_1) \\ \tilde{\Upsilon}_{24} &= (\sigma_1 \tau_1 \rho_1 \mu_2, \sigma_2 \tau_3 \rho_3 \mu_0, \sigma_3 \tau_1 \rho_1 \mu_2) \\ \tilde{\Upsilon}_{25} &= (\sigma_1 \tau_2 \rho_1 \mu_2, \sigma_2 \tau_3 \rho_3 \mu_0, \sigma_3 \tau_2 \rho_1 \mu_2) \\ \tilde{\Upsilon}_{26} &= (\sigma_1 \tau_0 \rho_3 \mu_2, \sigma_2 \tau_3 \rho_3 \mu_0, \sigma_3 \tau_0 \rho_3 \mu_2) \\ \tilde{\Upsilon}_{27} &= (\sigma_1 \tau_3 \rho_3 \mu_3, \sigma_2 \tau_3 \rho_3 \mu_0, \sigma_3 \tau_3 \rho_3 \mu_3) \\ \tilde{\Upsilon}_{28} &= (\sigma_1 \tau_3 \rho_3 \mu_1, \sigma_2 \tau_3 \rho_3 \mu_1, \sigma_3 \tau_3 \rho_3 \mu_0) \\ \tilde{\Upsilon}_{29} &= (\sigma_1 \tau_1 \rho_1 \mu_2, \sigma_2 \tau_1 \rho_1 \mu_2, \sigma_3 \tau_3 \rho_3 \mu_0) \\ \tilde{\Upsilon}_{30} &= (\sigma_1 \tau_2 \rho_1 \mu_2, \sigma_2 \tau_2 \rho_1 \mu_2, \sigma_3 \tau_3 \rho_3 \mu_0) \\ \tilde{\Upsilon}_{31} &= (\sigma_1 \tau_0 \rho_3 \mu_2, \sigma_2 \tau_0 \rho_3 \mu_2, \sigma_3 \tau_3 \rho_3 \mu_0) \\ \tilde{\Upsilon}_{32} &= (\sigma_1 \tau_3 \rho_3 \mu_3, \sigma_2 \tau_3 \rho_3 \mu_3, \sigma_3 \tau_3 \rho_3 \mu_0) \\ \tilde{\Upsilon}_{33-35} &= (\sigma_0 \tau_1 \rho_1 \mu_1, \sigma_i \tau_1 \rho_1 \mu_2, \sigma_i \tau_3 \rho_3 \mu_3) \\ \tilde{\Upsilon}_{36} &= \sigma_0 (\tau_1 \rho_1 \mu_1, \tau_3 \rho_3 \mu_2, \tau_1 \rho_1 \mu_3) \\ \tilde{\Upsilon}_{37-39} &= (\sigma_0 \tau_2 \rho_1 \mu_1, \sigma_i \tau_2 \rho_1 \mu_2, \sigma_i \tau_3 \rho_3 \mu_3) \\ \tilde{\Upsilon}_{40} &= \sigma_0 (\tau_2 \rho_1 \mu_1, \tau_3 \rho_3 \mu_2, \tau_2 \rho_1 \mu_3) \end{aligned}$$

| Y_i | $\mathcal{T}(\sigma_0)$ | D_6 | Φ for σ_0 in Y_i | Φ for σ in Y_i |
|------------------------------------|-------------------------|--------------|--|------------------------------|
| $\sigma_\mu(\tau_1, \tau_2)\rho_1$ | + | (A_1, B_1) | $\sigma_0\tau_0\rho_0$ | - |
| $\sigma_\mu\tau_0\rho_3$ | + | B_2 | $\sigma_0\tau_0\rho_0, \sigma\tau_3\rho_0$ | - |
| $\sigma_\mu\tau_3\rho_3$ | - | A_2 | - | $\sigma_0\tau_0\rho_0$ |

Table I. Coupling matrices for WSe_2 that anti-commute with the $\alpha_{1,2}$, along with their transformation under time-reversal (we list the charge sector (σ_0), the spin sector (σ) transforms oppositely) and the transformation under D_6 . The pairing states for the charge and spin sector bosons are listed in the last two columns. Only time-reversal even interactions cause superconductivity. Two TIVC states in the first row are grouped into a pair that transforms into each other under $U_v(1) = \exp(i\zeta\tau_3)$, i.e. they approximately behave like XY degrees of freedom. Individually, each would also induce another triplet state (not listed), for which the other XY component is however repulsive.

| Y_i | $\mathcal{T}(\sigma_0)$ | D_6 | Φ for σ_0 in Y_i | Φ for σ in Y_i |
|---|-------------------------|--------------|--|--|
| $\sigma_\mu(\tau_1, \tau_2)\rho_1\mu_1$ | + | (A_1, B_1) | $\sigma_0\tau_0\rho_0\mu_{0,1}, \sigma_0\tau_3\rho_0\mu_2,$ $\sigma\tau_3\rho_0\mu_3$ | $\sigma_0\tau_0\rho_0\mu_3$ |
| $\sigma_\mu(\tau_1, \tau_2)\rho_1\mu_2$ | - | (A_2, B_2) | $\sigma_0\tau_0\rho_0\mu_{1,3}, \sigma_0\tau_3\rho_0\mu_2,$ $\sigma\tau_3\rho_0\mu_0$ | $\sigma_0\tau_0\rho_0\mu_0$ |
| $\sigma_\mu(\tau_1, \tau_2)\rho_1\mu_3$ | + | (A_2, B_2) | $\sigma_0\tau_0\rho_0\mu_{0,3}, \sigma_0\tau_3\rho_0\mu_2,$ $\sigma\tau_3\rho_0\mu_1$ | $\sigma_0\tau_0\rho_0\mu_1$ |
| $\sigma_\mu(\tau_1, \tau_2)\rho_1\mu_0$ | + | (A_1, B_1) | $\sigma_0\tau_0\rho_0\mu_{0,1,3}, \sigma\tau_0\rho_0\mu_2$ | $\sigma_0\tau_3\rho_0\mu_2$ |
| $\sigma_\mu\tau_0\rho_3\mu_0$ | + | B_2 | $\sigma_0\tau_0\rho_0\mu_{0,1,3}, \sigma_0\tau_3\rho_0\mu_2,$ $\sigma\tau_3\rho_0\mu_{0,1,3}, \sigma\tau_0\rho_0\mu_2$ | $\sigma_0\tau_{1,2}\rho_2\mu_2$ |
| $\sigma_\mu\tau_3\rho_3\mu_0$ | - | A_2 | - | $\sigma_0\tau_0\rho_0\mu_{0,1,3}, \sigma_0\tau_3\rho_0\mu_2,$ $\sigma_0\tau_{1,2}\rho_2\mu_2$ |
| $\sigma_\mu\tau_0\rho_3\mu_1$ | + | B_2 | $\sigma_0\tau_0\rho_0\mu_{0,1}, \sigma_0\tau_{1,2}\rho_2\mu_2,$ $\sigma\tau_3\rho_0\mu_{0,1}, \sigma\tau_{1,2}\rho_2\mu_3$ | $\sigma_0\tau_3\rho_0\mu_2, \sigma_0\tau_0\rho_0\mu_3$ |
| $\sigma_\mu\tau_3\rho_3\mu_2$ | + | A_1 | $\sigma_0\tau_0\rho_0\mu_0, \sigma_0\tau_3\rho_0\mu_2,$ $\sigma_0\tau_{1,2}\rho_2\mu_2, \sigma\tau_0\rho_0\mu_2,$ $\sigma\tau_3\rho_0\mu_0, \sigma\tau_{1,2}\rho_2\mu_0$ | $\sigma_0\tau_0\rho_0\mu_{1,3}$ |
| $\sigma_\mu\tau_3\rho_3\mu_1$ | - | A_2 | $\sigma_0\tau_3\rho_0\mu_2, \sigma_0\tau_0\rho_0\mu_3,$ $\sigma_0\tau_{1,2}\rho_2\mu_2, \sigma\tau_0\rho_0\mu_2,$ $\sigma\tau_3\rho_0\mu_3, \sigma\tau_{1,2}\rho_2\mu_3$ | $\sigma_0\tau_0\rho_0\mu_{0,1}$ |
| $\sigma_\mu\tau_0\rho_3\mu_2$ | - | B_1 | $\sigma_0\tau_0\rho_0\mu_{1,3}, \sigma_0\tau_{1,2}\rho_2\mu_2,$ $\sigma\tau_{1,2}\rho_2\mu_0, \sigma\tau_3\rho_0\mu_{1,3}$ | $\sigma_0\tau_0\rho_0\mu_0, \sigma_0\tau_3\rho_0\mu_2$ |
| $\sigma_\mu\tau_0\rho_3\mu_3$ | + | B_1 | $\sigma_0\tau_0\rho_0\mu_{0,3}, \sigma_0\tau_{1,2}\rho_2\mu_2,$ $\sigma\tau_{1,2}\rho_2\mu_1, \sigma\tau_3\rho_0\mu_{0,3}$ | $\sigma_0\tau_0\rho_0\mu_1, \sigma_0\tau_3\rho_0\mu_2$ |
| $\sigma_\mu\tau_3\rho_3\mu_3$ | - | A_1 | $\sigma_0\tau_0\rho_0\mu_1, \sigma_0\tau_3\rho_0\mu_2,$ $\sigma_0\tau_{1,2}\rho_2\mu_2, \sigma\tau_3\rho_0\mu_1,$ $\sigma\tau_{1,2}\rho_2\mu_1, \sigma\tau_0\rho_0\mu_2$ | $\sigma_0\tau_0\rho_0\mu_{0,3}$ |

Table II. Same as Table I but for TBG. The first two lines correspond to TIVC and KIVC, respectively. These IVCs are listed as two-component order parameters as they transform into each other under the broken $U_v(1) = \exp(i\zeta\tau_3)$, i.e. they approximately behave like XY degrees of freedom. For mini-valleys, intravalley (intervalley) states with μ_1 , and μ_2 (μ_0 and μ_3) can also be grouped together as they transform into each other under translational symmetry on the moiré scale, in analogy to the $\tau_{1,2}$ states and graphene-scale translational symmetry. These pairs are indicated by the dashed lines between them. If we assume they appear together, this would reduce the number of pairing states: only states occur in both rows remain.

$$\begin{aligned}
\vec{Y}_{41-43} &= (\sigma_0\tau_0\rho_3\mu_1, \sigma_i\tau_0\rho_3\mu_2, \sigma_i\tau_3\rho_3\mu_3) \\
\vec{Y}_{44} &= \sigma_0(\tau_0\rho_3\mu_1, \tau_3\rho_3\mu_2, \tau_0\rho_3\mu_3) \\
\vec{Y}_{45-47} &= (\sigma_0\tau_1\rho_1\mu_3, \sigma_i\tau_1\rho_1\mu_2, \sigma_i\tau_3\rho_3\mu_1) \\
\vec{Y}_{48-50} &= (\sigma_0\tau_2\rho_1\mu_3, \sigma_i\tau_2\rho_1\mu_2, \sigma_i\tau_3\rho_3\mu_1) \\
\vec{Y}_{51-53} &= (\sigma_0\tau_0\rho_3\mu_3, \sigma_i\tau_0\rho_3\mu_2, \sigma_i\tau_3\rho_3\mu_1) \\
\vec{Y}_{54-56} &= (\sigma_0\tau_3\rho_3\mu_2, \sigma_i\tau_3\rho_3\mu_1, \sigma_i\tau_3\rho_3\mu_3) \quad (B4)
\end{aligned}$$

Particularly interesting are those where at least some of the components transform into each other under either $SU(2)_{\text{spin}}$ or $U(1)_{\text{valley}}$, i.e. $\vec{Y}_1, \vec{Y}_{12}, \vec{Y}_{16}$ as well as \vec{Y}_{17} . The corresponding superconducting states can be obtained with the help

of Table II. Modulo a change of basis and taking into account that we only considered \vec{Y} where all components transform the same under time reversal, this is closely related to Table III in Ref. 34. Differences in the two tables are due to the fact that we do not group states into pairs w.r.t. the mini-valley. This would remove \vec{Y}_1 and \vec{Y}_{16} as options while adding a moiré density wave (second line in Table III of Ref. 34) as the third one. This third option can be directly obtained from Table II as

$$\vec{Y} = (\sigma_0\tau_0\rho_3\mu_1, \sigma_0\tau_3\rho_3\mu_2, \sigma_0\tau_0\rho_3\mu_3) \quad (B5)$$

which maps to the associated line in Ref. 34 upon basis transformation. The only compatible zero-momentum superconducting order parameter is the A_1 singlet.